Computers and Concrete, Vol. 5, No. 3 (2008) 243-260
DOI: http://dx.doi.org/10.12989/cac.2008.5.3.243

Characteristic features of concrete behaviour: Implications for the development of an engineering finite-element tool

Michael D. Kotsovos*

Laboratory of Concrete Structures, National Technical University of Athens, Greece

Milija N. Pavlovic and Demetrios M. Cotsovos

Department of Civil Engineering, Imperial College, London, USA

(Received April 10, 2007, Accepted June 23, 2008)

Abstract. The present article summarises the fundamental characteristics of concrete behaviour which underlie the formulation of an engineering finite element model capable of realistically predicting the behaviour of (plain or reinforced) concrete structural forms in a wide range of problems ranging from static to impact loading without the need of any kind of re-calibration. The already published evidence supporting the proposed formulation is complemented by four additional typical case studies presented herein; for each case, a comparative study is carried out between numerical predictions and the experimental data which reveals good agreement. Such evidence validates the material characteristics upon which the FE model's formulation is based and provides an alternative explanation regarding the behaviour of structural concrete and how it should be modelled which contradicts the presently (widely) accepted assumptions adopted in the majority of FE models used to predict the behaviour of concrete.

Keywords: brittle behaviour; concrete; constitutive law; static (monotonic and cyclic) and dynamic (earthquake and impact) loading; nonlinear finite element analysis; structural concrete.

1. Introduction

Most finite-element (FE) packages (e.g. ABAQUS, ADINA, LS-DYNA, etc) that may be used for the analysis of concrete structures under a wide range of loading conditions, extreme loading conditions such as those encountered in impact and explosion situations inclusive, rely on the use of constitutive models which place emphasis on the description of post-peak concrete characteristics such as, for example, strain softening, tension stiffening, shear-retention ability, etc, coupled with stress- and/or strain-rate sensitivity when blast or impulsive types of loading are considered. The derivations of such constitutive models has been based on a variety of theories, including plasticity (Malvar, *et al.* 1997, Thabet and Haldane 2001), viscoplasticity (Cela 1998, Winnicki, *et al.* 2001, Gomes and Awruch 2001, Georgin and Reynouard 2003, Barpi 2004), continuum damage mechanics (Cervera, *et al.* 1996, Hatzigeorgiou, *et al.* 2001, Koh, *et al.* 2001, Lu and Xu 2004) or a combination of these theories (Dube, *et al.* 1996, Faria, *et al.* 1998).

* Professor, Corresponding Author, E-mail: mkotsov@central.ntua.gr

However, the application of FE packages in practical structural analysis has shown that such constitutive relationships are case-study dependent, since the solutions obtained are realistic only for particular problems such as, for example, reinforced-concrete (RC) walls (Agrawal, *et al*. 1981, Dube, *et al.* 1996, Ile and Reynouard 2000, Faria, *et al.* 2002) and RC frames (Mochida, *et al*. 1987, Lee and Woo 2002) under earthquake loading, plain-concrete prisms or cylinders (Tedesco, *et al.* 1989, 1991 and 1997, Georgin and Reynouard 2003, Koh, *et al* 2001, Thabet and Haldane 2001, Gomes and Awruch 2001), RC beams (Dube, *et al.* 1996), RC walls (Malvar, *et al.* 1997), RC slabs (Cela 1998) and RC plates (Sziveri, *et al.* 1999) under impact loading, etc; in order to extend, therefore, the applicability of the packages to a different set of problems requires modifications, sometimes significant, of the constitutive relationships. The cause of the above apparent lack of generality is considered to mainly relate, on the one hand, to the misinterpretation of the observed material behaviour and, on the other, to the use of experimental data of questionable validity for the calibration of the constitutive relationships.

To this end, the work presented in the paper is intended to summarise the main findings of already published work which shows that the use of valid experimental data can lead to the development of a simple model of concrete behaviour enabling FE analysis to yield realistic solutions for a wide range of practical problems covering both short-term static and dynamic (earthquake and impact) loading conditions. The presently adopted FE model has been successfully used in a large number of case studies investigating the behaviour of a wide range of plain and reinforced structural forms (i.e. cylindrical and prismatic plain concrete specimens, beams, slabs, walls, frames etc) under static monotonic loading (an extensive literature review on the publications concerning such case studies – over 30 – is presented by Kotsovos and Pavlovic 1995). Its applicability however, has recently been extended to static cyclic loading and dynamic loading ranging from earthquake to impact (Cotsovos 2004). In all cases the numerical and the corresponding experimental data show good agreement thus validating the material characteristics and numerical procedure upon which its formulation is based. The concepts, and, in particular, the fundamental features of concrete behaviour which underlie the development of the above FE model are first discussed and then additional results extracted from four typical case studies (which form the subject of ongoing research) are presented as further evidence of the validity of these concepts.

2. Fundamental concrete characteristics

Brittle post-peak behaviour: The experimental data on concrete behaviour used for the development of constitutive laws are obtained from tests on specimens such as, for example, cylinders, prisms, cubes, etc. Such specimens are subjected to various load combinations, usually applied (at least in one of the three principal directions) through rigid steel platens; the results obtained are expressed in the form of stress-strain curves which comprise a strain hardening branch followed by a strain softening one, the latter widely considered to be essential in ultimate limit-state analysis and design. And yet, it has been known since the early 80s (Kotsovos 1983, van Mier 1986), and confirmed in the late 90s in the report by the relevant RILEM Technical Committee (van Mier, *et al*. 1997), that only strain hardening may describe material behaviour under a definable state of stress; strain softening merely reflects the interaction between specimen and testing device, which, for the case of a predominantly compressive state of stress, is effected through the development of indefinable frictional stresses at the end faces of the specimen. In fact, it has been shown (Kotsovos 1983) that

the rate of reduction of the residual concrete strength with increasing strain increases rapidly as the means to reduce the above frictional stresses becomes more effective. Such behaviour indicates that were the frictional stresses completely eliminated, concrete would be characterised by a complete and immediate loss of load-carrying capacity as soon as the peak load level is attained.

Stress path independency: Decomposing the stress-strain behaviour of concrete under any state of monotonically-increasing stress into hydrostatic and deviatoric components yields stress-strain curves which are expressed in the form of normal and shear octahedral stresses (σ_o and τ_o) and strains (γ_o and ε_o). These curves show that, while under hydrostatic stress only ε_0 varies with σ_o, under deviatoric stress both γ_o and ε_o vary with τ_o (Kotsovos and Pavlovic 1995). More importantly, however, it has been shown experimentally that such curves exhibit a statistically insignificant deviation from the curves established from tests on specimens subjected to either pure hydrostatic or pure deviatoric states of stress (Kotsovos 1984). Such a small deviation indicates that the deformational behaviour of concrete is essentially stress-path independent (Kotsovos and Pavlovic 1995). A similar conclusion has also been drawn from the analysis of experimental data on concrete strength (Kotsovos and Pavlovic 1995).

"Poisson's ratio" effect: The development of most (though not all) constitutive relations of concrete behaviour published to date has been directly or indirectly based on the assumption of a constant value of the Poisson's ratio (PR) or that this important parameter takes values near failure that are considerably less than the true ones. However, such an assumption is in conflict with experimental data which show that the PR is essentially constant up to a value of the applied load equal to between approximately 30% and 50% of the peak load level; and that, beyond this load level, the PR increases at an increasing rate and attains a value that becomes significantly larger than 0.5 when the peak load level is reached (Barnard 1964). Such behaviour clearly indicates that concrete ceases to be a continuum beyond a load level close to, but not beyond, the peak load, a fact consistent with the material's brittle nature.

Cracking: Cracking occurs in localised regions of an RC structural element in order to relieve tensile stresses when the material strength in tension is attained. The crack faces coincide with the plane of the maximum and intermediate principal stresses (assuming compression as positive) and opens in the orthogonal direction (i.e. in the direction of the minimum principal compressive stress or maximum principal tensile stress), whereas its extension occurs in the direction of the maximum principal compressive stress (Kotsovos and Pavlovic 1995). Such a cracking mechanism precludes any shearing movement of the crack faces and, therefore, contrasts widely adopted mechanisms of shear resistance such as, for example, aggregate interlock and dowel action, which can only be mobilised through the "shearing" movement of the crack faces.

Loading-rate independency: The vast majority of existing constitutive models used for describing the behaviour of concrete under high rates of loading are based on the assumption that there is a link between the mechanical properties of concrete and the rate at which the loading is imposed ("loading-rate sensitivity"). However, it has recently been suggested that loading-rate sensitivity is based on an uncritical interpretation of the available experimental data, the latter describing structural, rather than material, response (Cotsovos 2004). In the present work, the mechanical properties of concrete are considered to be independent of the loading rate, with the effect of the latter on the specimen behaviour being primarily attributed to the inertia effect of the specimen mass: this simple (and, arguably, obvious – though, at present, unorthodox) postulate was the subject of a numerical investigation which proved it capable of reproducing the experimental data available from past tests (Cotsovos 2004). Moreover, this numerical investigation confirmed the

importance and significance of the role that inertia plays in the specimen's response when subjected to high rates of loading.

3. Use in finite-element analysis

3.1. Constitutive law of concrete behaviour

A constitutive law of concrete behaviour (fully defined by a single material parameter - the uniaxial cylinder compressive strength f_c) with the characteristics described above is described in detail in Kotsovos and Pavlovic (1995), and, therefore, it is only briefly discussed in the following.

Stress-strain behaviour: Its analytical description has been based on an analysis of triaxial experimental stress-strain data expressed in the form octahedral normal and shear stresses (σ_o, τ_o) and strains (ε_o, γ_o). The variations of the secant and tangent values of the bulk modulus, $K_S = \sigma_o/\varepsilon_o$ and $K_T=d\sigma_o/d\varepsilon_o$, respectively, with σ_o may easily be established from σ_o-ε_o curves and expressed in the form graphically represented in Fig. 1(a). Similarly, the variations of the secant and tangent values of the shear modulus, $G_S = \tau_o/\gamma_o$ and $G_T = d\tau_o/d\gamma\varepsilon_o$, respectively, with τ_o may easily be established from τ_o-γ_o curves and expressed in the form graphically represented in Fig. 1(b). In Figs. 1(a) and 1(b), both modulae are normalised with respect to their tangent values (K_e and G_e) at the origin of the stress-strain curves, the latter values being essentially the elastic values, which has been shown to adequately describe material behaviour during unloading (Kotsovos and Pavlovic 1995). Moreover, the variation of ε_o with τ_o for a given σ_o – expressing the coupling between the hydrostatic and deviatoric components of stress and strain – is transformed into the variation of an *internal hydrostatic stress* σ_{int} with τ_o for a given σ_o, which is shown in Fig. 1(c) (Kotsovos and Pavlovic 1995). Stress σ_{int}, which represents the reduction caused by cracking to the internal tensile stresses, only develops during loading, as unloading does not cause any cracking and hence σ_{int} = 0. Having expressed K_S (K_T) and G_S (G_T) as functions of σ_o and τ_o, respectively, and σ_{int} as a function of σ_o and τ_o, the strains corresponding to a given state of stress is easily obtained from Hooke's law by adding σ_{int} to σ_o (Kotsovos and Pavlovic 1995).

Failure criterion: As for the case of the deformational properties, the analytical description of the failure criterion (strength surface) has also been based on a regression analysis of valid experimental data expressed in the form indicated in Fig. 2. Such data were used for the analytical description of the strength-surface meridians corresponding to θ=0^o (σ_1=$\sigma_2 \geq \sigma_3$) and θ=60^o and ($\sigma_1 \geq \sigma_2$=σ_3) graphical representations of the resulting expressions are also shown in Fig. 2 (Kotsovos and Pavlovic 1995). For meridians corresponding to a value of the rotational variable θ between 0^o and 60^o the interpolation function derived by Willam and Warnke (1974) may be used.

3.2. Constitutive law for steel bars

The constitutive model used to describe the behaviour of steel reinforcement uses the simple form indicated in Fig. 3, where the stress-strain curve describes the behaviour of a steel bar under uniaxial compression or tension. It is divided into three linear sections. In each one of these sections, the material properties remain constant. The first and second sections of the stress-strain diagram are defined by the yield stress. The third section starts from the point where the stress is equal to the yield stress f_y and has a very small inclination, usually 1% of the slope of the first elastic section. As a result, small increases in

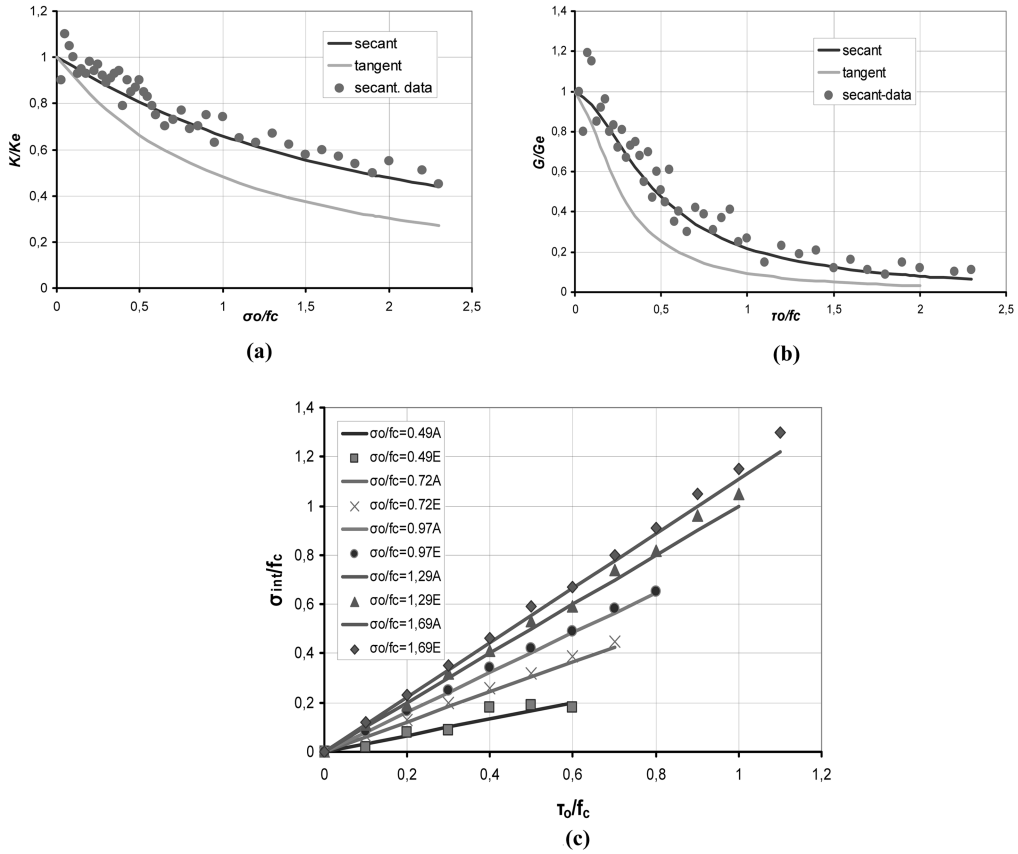

Fig. 1 Variations of : (a) secant (K_S) and tangent (K_T) values of the bulk modulus with σ_o; (b) secant (G_S) and tangent (G_T) values of the shear modulus with τ_o; and (c) internal stress state intwith σ_o and τ_o

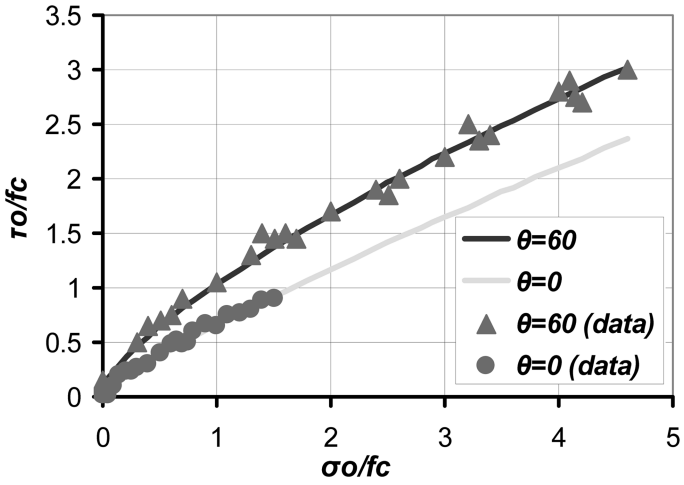

Fig. 2 Typical strength surface meridians corresponding to θ^o= 0^o and θ^o=60^o

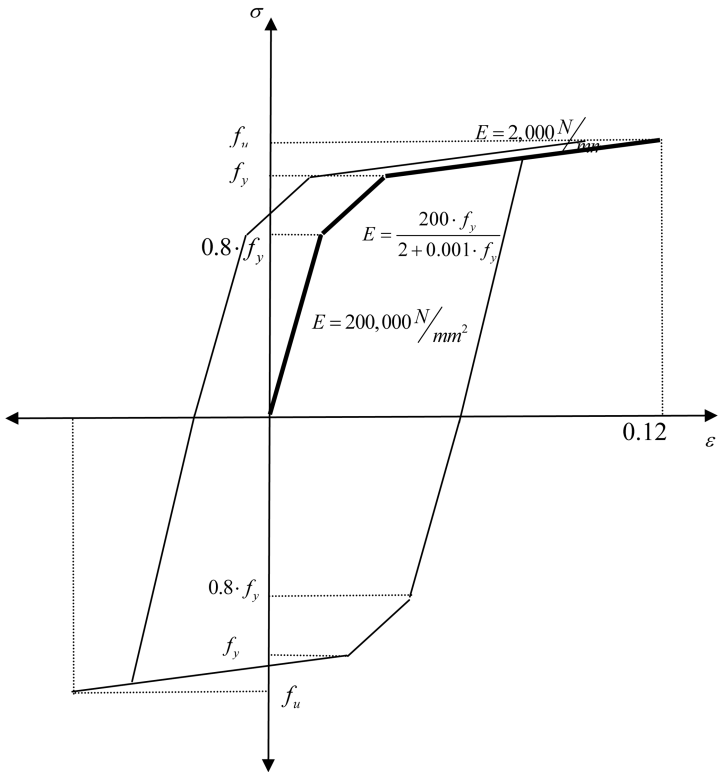

Fig. 3 Graphical representation of constitutive model for steel reinforcement

stress cause large increases in strain. The steel-reinforcement fails when the strain attains its ultimate value ε_u. Fig. 3 also depicts how load reversals can be accommodated by the stress-strain relations adopted for the reinforcement bars.

3.3. Concrete-steel interaction

It is considered that the concrete-steel interaction is adequately described by the assumption of perfect bond. The key argument for adopting this assumption is that the tensile strength of concrete is significantly lower than the value of the shear stress that causes bond failure on the basis of experimental evidence cited in Kotsovos and Pavlovic (1995), and, hence, the formation of a crack due to tensile failure of concrete will occur before the maximum shear stress predicted by any of the bond-slip laws adopted to date is attained.

3.4. Finite-element solution procedure

The implementation in structural analysis of a constitutive law of concrete behaviour with the above characteristics was achieved through the development of a finite-element (FE) package that is briefly described herein as its full details may be found elsewhere (Kotsovos and Pavlovic 1995, Kotsovos and Spiliopoulos 1998a,b, Cotsovos 2004). This package, used in the past to predict the nonlinear behaviour of a wide range of RC structural forms under static monotonic loading

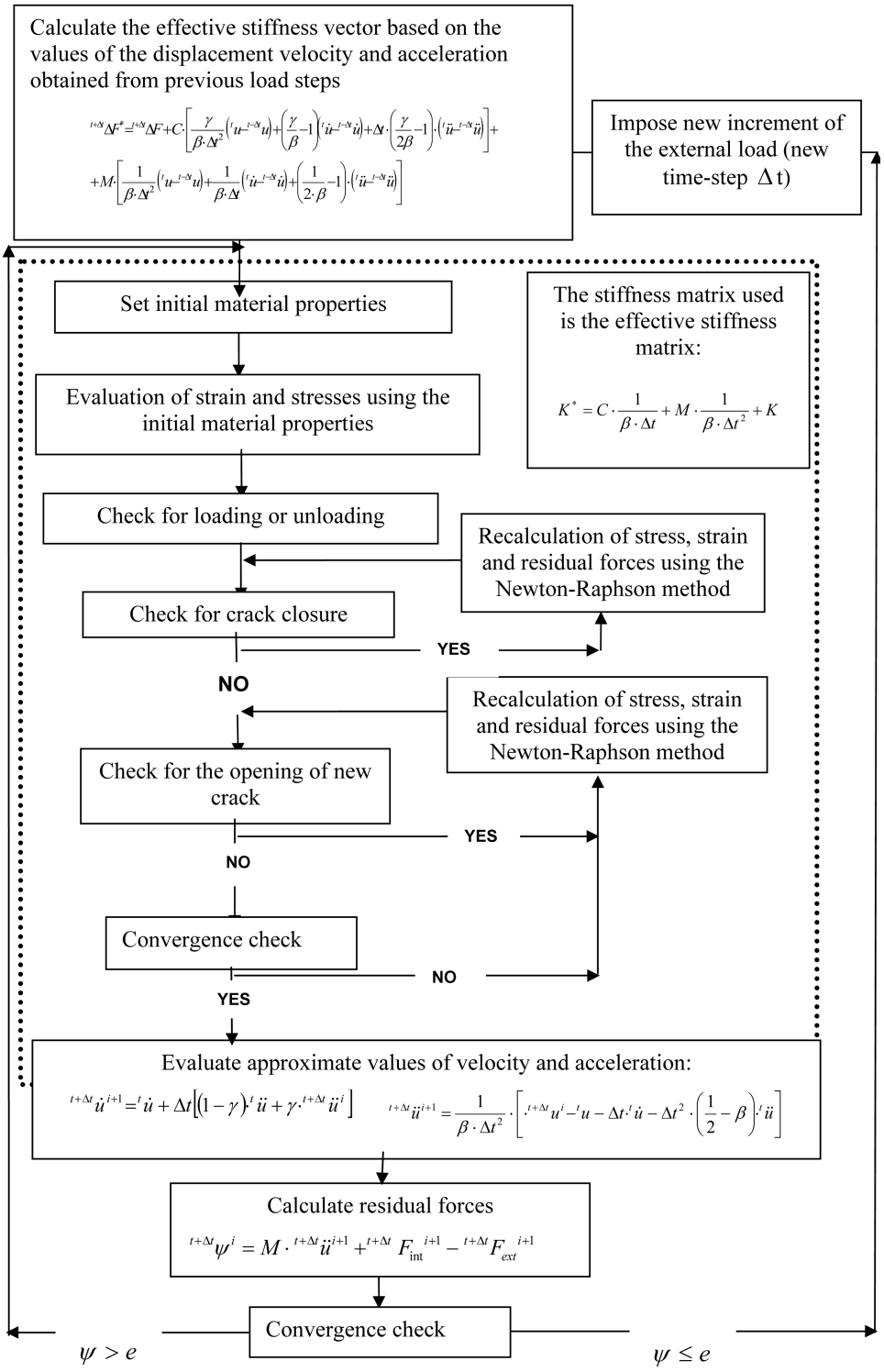

Fig. 4 Nonlinear iterative procedure

(Kotsovos and Pavlovic 1995) has now been extended to dynamic problems (Cotsovos 2004). Owing to the complexity of the nonlinear behaviour of concrete and steel, as well as their interaction, the equation of motion is solved numerically by using the FE method and the Newmark family of approximations (Bathe 1996). An implicit scheme, usually associated with problems with a longer duration, such as earthquake problems, and the unconditionally stable average-acceleration method are used throughout.

The nonlinear iterative procedure adopted for solving the nonlinear dynamic problem is concisely described in Fig. 4 (Cotsovos 2004). In essence the nonlinear dynamic problem is viewed as a sequence of equivalent static problems. At the beginning of each iteration and based on the values of displacement, velocity and acceleration obtained from the previous iteration, the effective stiffness and load matrices are calculated and an equivalent static problem is formulated. The solution procedure adopted for the equivalent static problem – described within the dotted line in Fig. 4 – is an iterative procedure on its own and its formulation is based on a modified Newton-Raphson procedure described in detail in Kotsovos and Pavlovic (1995). This procedure is the same as the one used for when dealing with static problems (in which the actual stiffness and load matrices are used instead of their effective counterparts). A characteristic feature of the solution process of the equivalent static problem is that every Gauss point is checked, at first, in order to determine whether loading or unloading takes place, and then in order to establish whether any cracks close or form. A crack is considered to close when the strain normal to its plane becomes compressive, whereas crack formation, occurring as described in section 2.4, is modelled by using the smeared crack approach (Kotsovos and Pavlovic 1995).

3.5. FE modelling

Concrete is modelled by using 20-node isoparametric or 27-node Lagrangian brick elements whereas, for steel reinforcement, a 3-node isoparametric truss element is adopted. As regards the size of the brick elements, this is such that the region corresponding to a Gauss point is kept to a size of approximately two times the size of the aggregate. This is compatible with the investigation stemming from cylinder samples tested for material properties so that the assumption of isotropy is acceptable from an engineering view point (Kotsovos and Pavlovi 1995).

4. FE Predictions of structural-concrete behaviour

The validity of the above nonlinear FE package has been verified by comparing the numerical predictions with experimental data obtained from tests on a wide range of structural members subjected to various regimes of static and dynamic loading. Full details of these comparative studies are given elsewhere (Kotsovos and Pavlovic 1995, Kotsovos and Spiliopoulos 1998a,b, Jelic, *et al.* 2004, and Cotsovos 2004). An indication of the predictive capabilities of the package is provided in the following by complementing the above comparative studies with four additional ones, which form part of ongoing research projects on the behaviour of typical RC structural members under loading regimes varying from short-term static to dynamic and short-term static to periodic.

4.1. Hinged beam under static monotonic loading

The beam selected for the present case study is the hinged beam C2 tested by Hughes and Speirs (1982), since, as discussed in section 4.2, similar beams have also been tested under impact loading. The beam, with a clear span of 2700 mm and a rectangular cross-section 200 mm (height)×100 mm (width), was reinforced with two 12 mm diameter compression bars, two 6 mm diameter tension bars, and 6 mm diameter stirrups at an approximately 180 mm centre-to-centre spacing (see Fig. 5 (top)). The modulus of elasticity (E_S), yield stress (f_y), and ultimate strength (f_u) of both the longitudinal and transverse reinforcement bars used are 206 GPa, 460 MPa and 560 MPa, respectively, with the compressive strength (f_c) of the concrete used being approximately 45 MPa.

The beam was subdivided into 20 brick elements as shown in Fig. 5(bottom). The line elements representing the steel reinforcement were placed along successive series of nodal points in both vertical and horizontal directions. Since the spacing of these line elements was predefined by the location of the brick elements' nodes, their cross-sectional area was adjusted so that the total amount of both longitudinal and transverse reinforcement to be equal to the design values.

The external load was applied in the form of displacement increments at mid span and the main results obtained are presented in Fig. 6, which shows a close correlation between the predicted load-displacement curve and its experimentally-established counterpart.

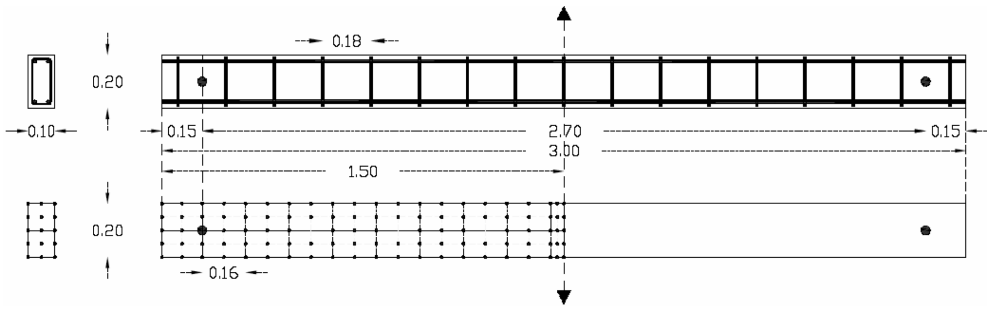

Fig. 5 Design details (top) and FE model (bottom) of hinged beams

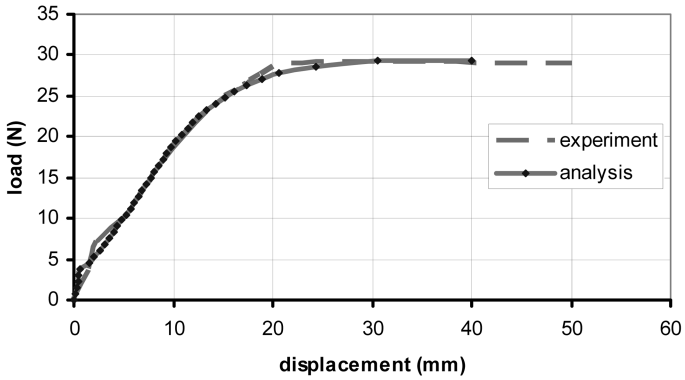

Fig. 6 Experimental and analytical load-deflection curves of beams in Figs 5 under static monotonic point loading

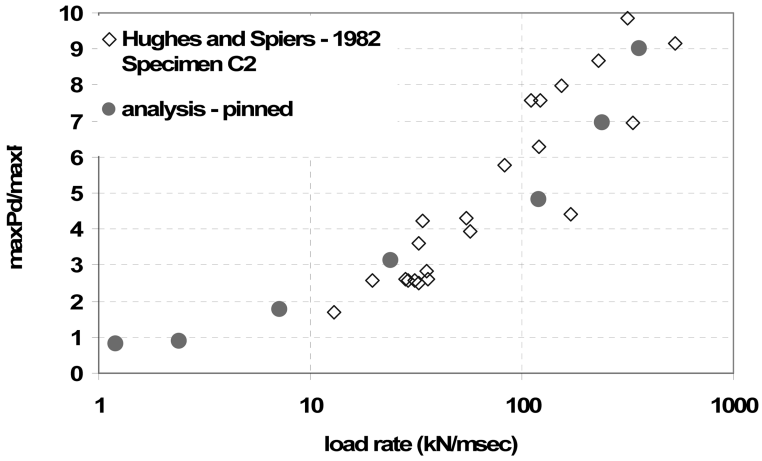

Fig. 7 Experimental and predicted variations of the $maxP_d/maxP_s$ ratio with the rate ofloading (where $maxP_d$ and $maxP_s$ are the values of load-carrying capacity under dynamic and static, respectively, loading)

4.2. Hinged beam under impact loading

As discussed in the preceding section, beam C2 is typical of a number of beams tested under loading applied at rates which vary from 1 kN/sec (static loading) to 10^7 kN/sec (impact loading).

For the case of impact loading, the load was applied by means of a steel mass left to fall onto the specimen from a certain height, depending on the desired rate of loading (Hughes and Speirs 1982, Miyamoto, *et al.* 1989, Kishi, *et al.* 2001, 2002). From the measured response, the beam's behaviour is characterised by an increase in load-carrying capacity with increasing loading rate (see Fig. 7). However, it is interesting to note in Fig. 7 the very large scatter exhibited by the test data. The cause of this scatter appears to predominantly reflect the difficulty in establishing experimentally the specimen load-carrying capacity under impact loading, with most values indicated in the figure usually exceeding the "true" load-carrying capacity by a significant margin. Hence, the trends of behaviour described by data such as those in the figure can only provide a qualitative, rather than quantitative, description of structural behaviour.

As for the case of static loading, the FE mesh adopted for the analysis is that depicted in Fig. 5, with the results obtained being also presented in Fig. 7, which shows that the analysis is capable of predicting trends of behaviour similar to those experimentally established.

4.3. Beam-column joint under cyclic loading

The present case has been extracted from a research programme concerned with an investigation of the validity of the methods currently used to design beam-column joints (Cotsovos and Kotsovos 2008). It involves an analytical study of the behaviour of one (designated as A2) of the beam-column joint specimens tested under cyclic loading by Shiohara and Kusuhara (2007) (see Fig. 8). The specimen was designed so as to exhibit over-strength of the beam-column joint, with the beam attaining its flexural capacity before the column; as a result, the storey shear was expected to reach its peak value when the beam attained its flexural capacity.

The design details of the specimen are shown in Fig. 9. The longitudinal reinforcement in both

the beams and the columns comprises 13 mm diameter bars (D13) with a nominal cross sectional area of 139 mm^2 and a yield stress (f_y) of 456.4 MPa, in the beams, and 356.9 MPa in the columns. For both beams and columns, the transverse reinforcement comprises 6 mm diameter stirrups (D6) (nominal cross-sectional area of 32 mm^2 and yield stress of 325.6 MPa) with a spacing of 50 mm. The mean compressive strength of concrete was 28 MPa. Full design details together with a comprehensive description of the mechanical properties of the materials used is provided elsewhere (Shiohara and Kusuhara 2007). At the location shown in Fig. 8, the specimen was subjected to the combined action of a constant axial load equal to 216 kN and a lateral displacement which was progressively increased in a cyclic manner to failure.

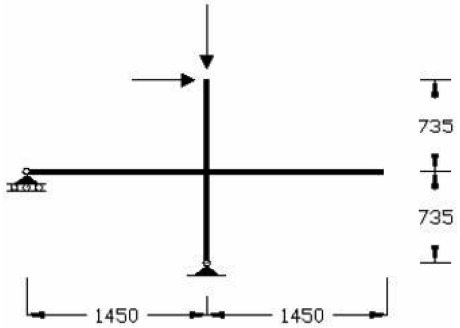

Fig. 8 Beam-column joint element investigated

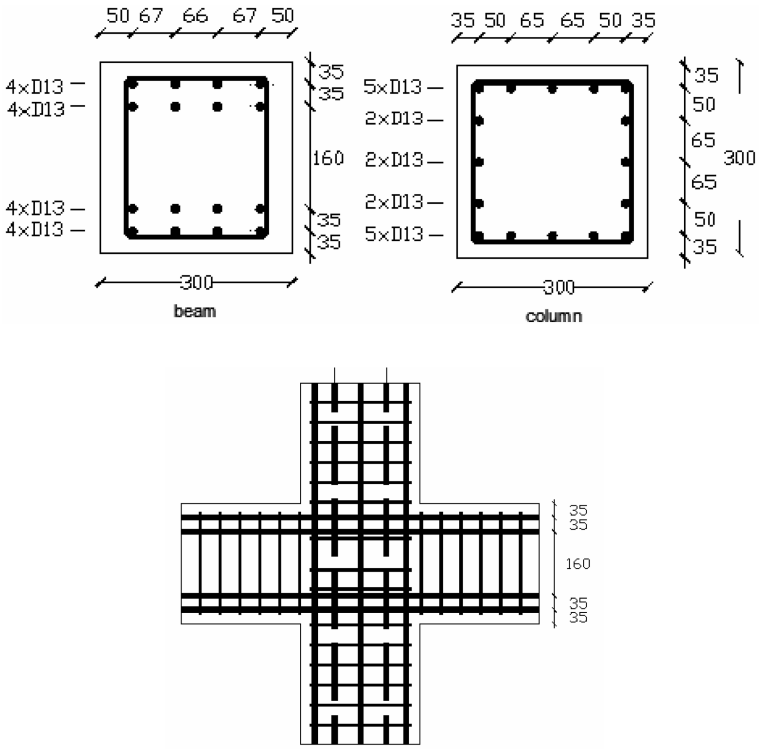

Fig. 9 Design details of beam-column joint element

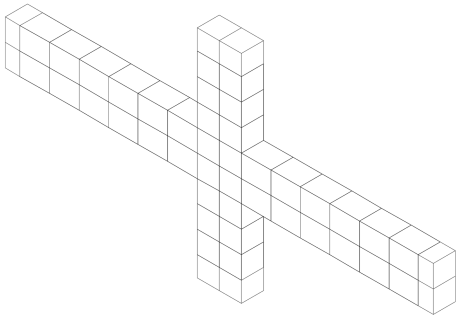

Fig. 10 FE model adopted for the analysis of the beam-column joint element

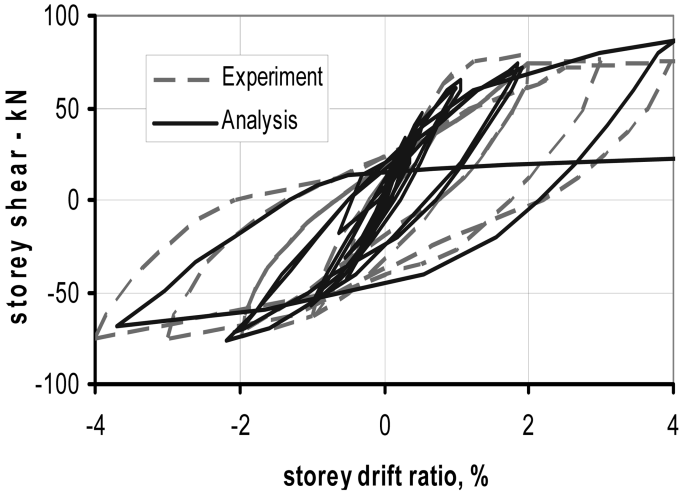

Fig. 11 Experimental and analytical storey shear vs. storey drift ratio curves for the beam-column joint element investigated (storey drift ratio is the ratio of the horizontal displacement of the loaded point to the length of the vertical member of the specimen in Fig. 8)

The beam-column joint was subdivided into 48 elements as shown in Fig. 10. The load was applied through a steel prismatic element monolithically connected to the upper end face of the column element; this steel element was subdivided into 2×1×1=2 brick FE elements, as indicated also in Fig. 10. The line elements representing the steel reinforcement were placed along successive series of nodal points in both vertical and horizontal directions. Since the spacing of these line elements was predefined by the location of the brick elements' nodes, their cross-sectional area was adjusted so that the total amount of both longitudinal and transverse reinforcement to be equal to the design values.

The results of the analysis, expressed in the form of a storey shear vs. drift ratio relationship, are shown in Fig. 11, which, for purposes of comparison, also includes the experimentally-established story shear vs. drift ratio relationship. Although the analysis method adopted does not allow for P-effects (which are clearly present in the case investigated), Fig. 11 indicates that the correlation between analytical and experimental results is realistic, with the area enclosed by the hysteretic loops of the analytically predicted storey shear-drift ratio curve being similar with its experimentally established counterpart.

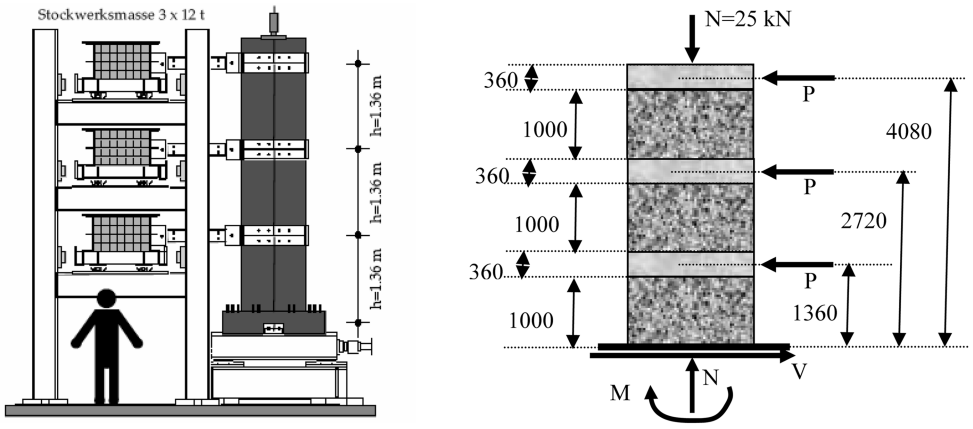

(a)

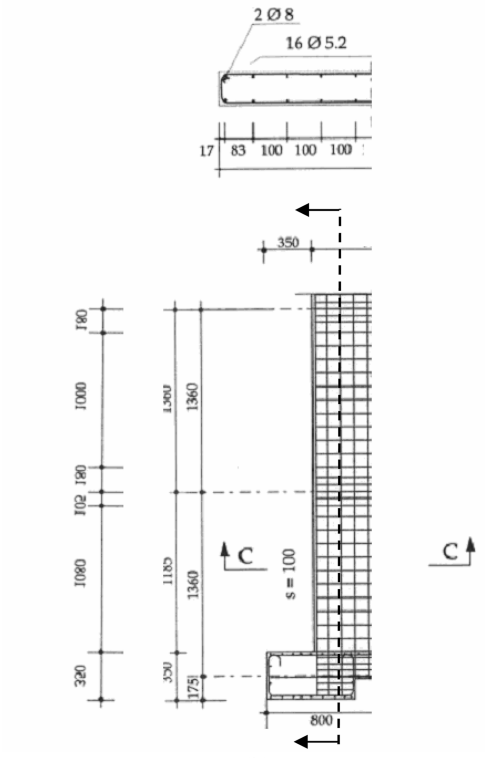

(b)

Fig. 12 Details for the RC wall under seismic excitation: (a) experimental setup (Lestuzzi, *et al.* 1999) (b) external loading and reactions; (c) arrangement of longitudinal and transverse reinforcement (this figure only shows the arrangement of the reinforcement for the first two storeys, the arrangement for the third storey is identical to that of the second) (all dimensions are expressed in mm)

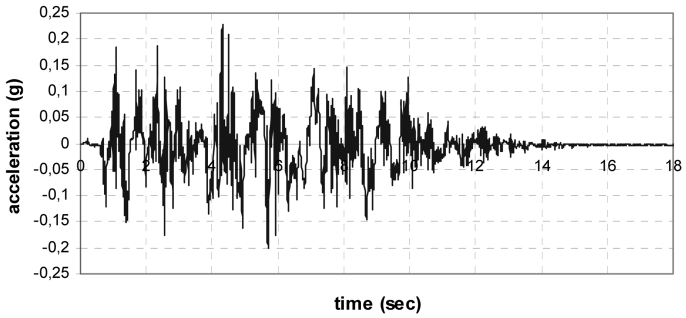

Fig. 13 Acceleration record used in the numerical and experimental investigation of the RCwall specimen in Fig. 12

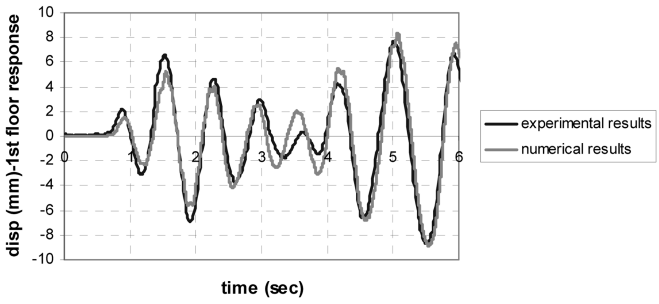

(a)

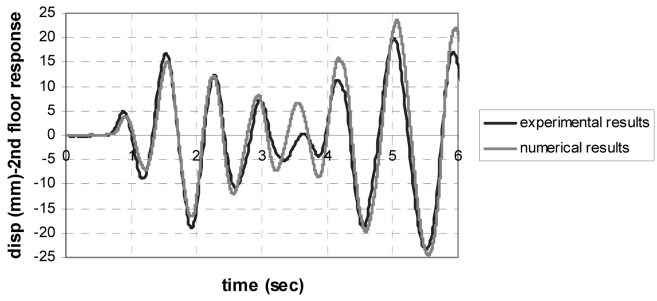

(b)

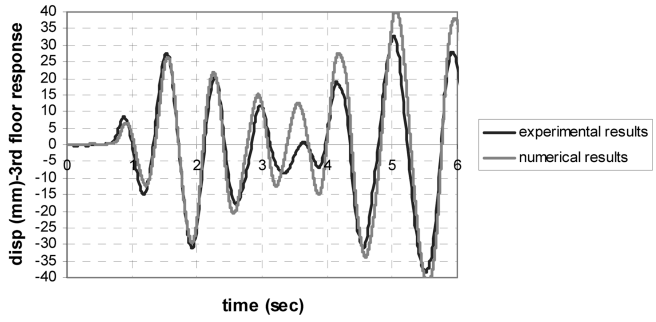

(c)

Fig. 14 Numerical and experimental displacement response of (a) the first floor (b) the second floor and (c) the third floor of the RC wall under seismic excitation

4.4. Three-storey structural wall under seismic excitation

Full details of the specimen and the test arrangement are provided elsewhere (Lestuzzi, *et al.* 1999). The RC wall had a cross-section of 900 mm×100 mm and a height of approximately 4 m. The wall corresponds to a three-story building and along its height three 12 ton masses were attached to it at approximately 1.36 m intervals as schematically shown in Fig. 12. Each mass (corresponding to the mass of a floor in the equivalent three-story building) was supported by a separate rigid steel three-story frame and was able to move only in the horizontal direction (so that the inertia of the masses affects only the horizontal motion of the structure). The wall was also subjected to uniaxial compressive loading, at approximately 30% of the axial compressive strength. A schematic representation of the RC wall tested and its design details are given in Fig. 12. The fc of the concrete was approximately 35 MPa. The values (in MPa) of the yield stress and ultimate strength (in parenthesis) of the reinforcement bars used were 567 (672), 483 (584), and 553 (611) for bar diameters (in mm) 8, 5 and 4, respectively.

Full details of the FE modelling and numerical predictions are given elsewhere (Cotsovos 2004, Cotsovos and Pavlovic 2004). Only the main results are presented herewith in a graphical form. The dynamic load was applied in the form of an acceleration record, which is presented in Fig. 13. The

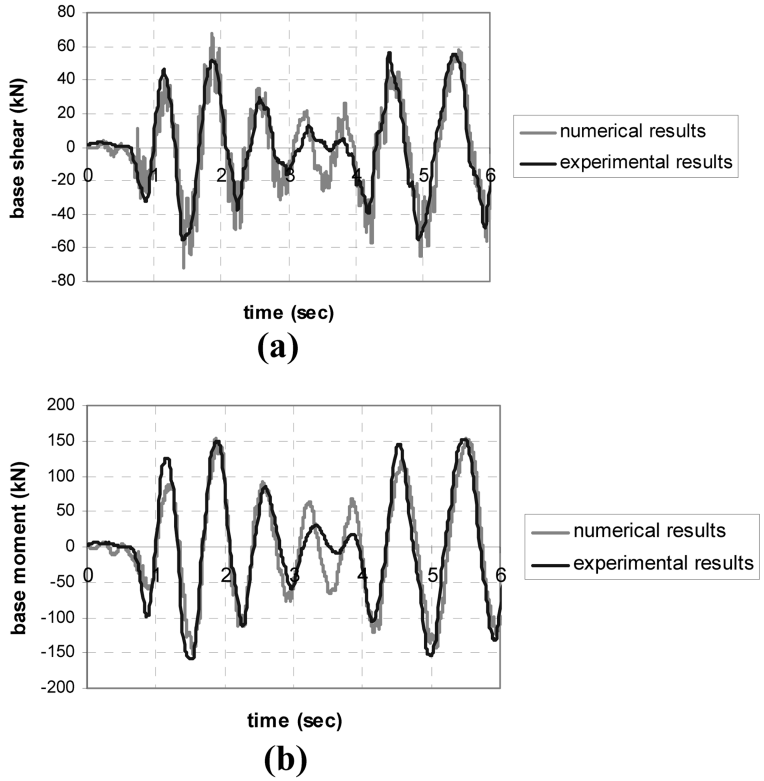

Fig. 15 Numerical and experimental (a) base shear and (b) base moment of the RC wall under seismic excitation

full response of the specimen during the experimental investigation is presented in Figs. 14 and 15 in the form of displacement-time and base shear/moment-time curves, respectively. It can be seen from the figures that the correlation between numerical predictions and measured values is very close in all cases.

5. Concluding remarks

It appears from the above that nonlinear FE analysis incorporating a brittle, triaxial model of concrete behaviour, load-path and loading-rate independent is capable of yielding realistic predictions for a wide range of structural-concrete configurations subjected to short-term loading conditions ranging from static and impact. Such evidence validates the concepts upon which the FE model's formulation is based and provides an alternative explanation regarding the behaviour of structural concrete and how it should be modelled which contradicts the presently (widely) accepted assumptions adopted by the majority of FE models used to predict concrete behaviour.

References

Agrwal, A. B., Jaeger, L.G. and Mufti, A. A. (1981), "Response of reinforced concrete shear walls under ground motions", *J. Struct. Div., ASCE*, **107**, 395-411.

Barnard, P. R. (1964), "Researches into the complete stress-strain curve for concrete", *Mag. Concrete Res.*, **16**(49), 203-210.

Barpi, F. (2004), "Impact behaviour of concrete: a computational approach", *Eng. Fracture Mech.* **71**, 2197-2213.

Bathe, K. J. (1996), *Finite Element Procedures*, Prentice Hall, New Jersey.

Cela, J. J. L. (1998), "Analysis of reinforced concrete structures subjected to dynamic loads with a viscoplastic Drucker-Prager model", *Appl. Math. Modelling* **22**, 495-515.

Cervera, M., Oliver, J. and Manzoli, O. (1996), "A rate-dependent isotropic damage model for the seismic analysis of concrete dams", *Earthq. Eng. Struct. Dyn.* **25**, 987-1010.

Cotsovos D. M. (2004), "Numerical Investigation of structural concrete under dynamic (Earthquake and Impact) loading", PhD thesis, University of London, UK

Cotsovos D. M. and Kotsovos M. D. (2008), "Cracking of RC beam/column joints: Implications for practical structural analysis and design", *The Structural Engineer*, **86**(12), 17 June.

Dube, J.-F., Pijaudier-Cabot, G. and La Borderie, C. (1996), "Rate dependent damage model for concrete in dynamics", *J. Eng. Mech. Div. ASCE*, **122**, 359-380.

Faria, R., Olivera, J. and Cervera, M. (1998), "A strain-based plastic viscous-damage model for massive concrete structures", *Int. J. Solids Struct.* **35**, 1533-1558.

Faria R., Vila Pouca N. and Delgado R. (2002), "Seismic behaviour of a R/C wall: Numerical simulation and experimental validation", *J. Earthq. Eng.*, **6**, 473-408.

Georgin, J. F. and Reynouard, J. M. (2003), "Modeling of structures subjected to impact: concrete behaviour under high strain rate", *Cement Concrete Compos.*, **217**, 131-143.

Gomes, H. M. and Awruch, A. M. (2001), "Some aspects on three-dimensional numerical modelling of reinforced concrete structures using the finite element method", *Advances in Eng. Software* **32**, 257-277.

Hatzigeorgiou, G., Beskos, D., Theodorakopoulos, D. and Sfakianakis, M. (2001), "A simple concrete damage model for dynamic FEM applications", *Int. J. Comput. Eng. Sci.*, **2**, 267-286.

Hughes, G. and Spiers, D. M. 1982, "An investigation on the beam impact problem", Cement and Concrete Association, Technical Report 546.

Ile, N. and Reynouard, J. M. 2000, "Nonlinear analysis of reinforced concrete shear wall under earthquake loading", *J. Earthq. Eng.*, **4**, 183-213.
Jelic, I., Pavlovic, M. N. and Kotsovos, M. D. (2004), "Performance of structural-concrete members under sequential loading and exhibiting points of inflection", *Comput. Concrete*, **1**(1), 99-113.
Kishi, N., Mikami, H. and Ando, T. (2001), "An applicability of the FE impact analysis on shear-failure-type RC beams with shear rebars". 4th Asia-Pacific Conference on Shock and Impact Loads on Structures. 309-315.
Kishi, N., Mikami, H., Matsuoka K. G. and Ando, T. (2002), "Impact behaviour of shear- failure-type RC beams without shear rebar", *Int. J. Impact Eng.*, **27**, 955-968.
Koh, C. G., Liu, Z. J. and Quek, S. T. (2001), "Numerical and experimental studies of concrete under impact", *Mag. Concrete Res.*, **53**, 417-427.
Kotsovos, M. D. (1983), "Effect of testing techniques on the post-ultimate behaviour of concrete in compression", *Mater. Struct., RILEM*, **16**(91), pp. 3-12.
Kotsovos M. D. and Pavlovic M. N. (1995), "Structural concrete: Finite-element analysis for limit-state design", Thomas Telford.
Kotsovos, M. D. and Spiliopoulos, K. V. (1998a), "Modelling of crack closure for finite-element analysis of structural concrete", *Comput. Struct.*, **69**, 383-398.
Kotsovos, M. D. and Spiliopoulos, K. V. (1998b), "Evaluation of structural-concrete design-concepts based on finite-element analysis", *Comput. Mech.*, **21**, 330-338.
Lee, H.-S. and Woo, S.-W. (2002), 'Seismic performance of a 3-story RC frame in a low-seismicity region", *Eng. Struct.*, **24**, 719-734.
Lestuzzi, P., Wenk, T. and Bachmann, H. (1999), "Dynamic tests of RC structural walls on the ETH earthquake simulator", IBK Report No. 240, Institüt für Baustatik und Konstruktion: ETH, Zurich.
Lu, Y. and Xu, K. (2004), "Modelling of dynamic behaviour of concrete materials under blast loading", *Int. J. Solids Struct.*, **41**, 131-143.
Malvar, L. J., Crawford, J. E, Wesevich, J. W. and Simons, D. (1997), "A plasticity concrete material model for DYNA3D", *Int. J. Impact Eng.*, **19**, 847-873.
Miyamoto, A., King, M. W. and Fujii, M. (1989), "Non-linear dynamic analysis and design concepts for RC beams under impulsive loads", *Bulletin of the New Zealand National Society for Earthquake Engineering*, **22**, 98-111.
Mochida, A., Mutsuyoshi, H. and Tsuruta, K. (1987), "Inelastic response of reinforced concrete frame structures subjected to earthquake motion", *Concrete Library of JSCE*, **10**, 125-138.
Shiohara, H. and Kusuhara, F. "Benchmark test for validation of mathematical models for nonlinear and cyclic behaviour of R/C beam-column joints", http://www.rcs.arch.t.utokyo.ac.jp/shiohara/benchmark/.
Sziveri, J., Topping, P. H. V. and Ivanyi, P. (1999), "Parallel transient dynamic non-linear analysis of reinforced concrete plates", *Advances Eng. Software*, **30**, 867-882.
Tedesco, J. W., Ross, A. C. and Brunair, R. M. (1989), "Numerical analysis of dynamic split cylinder tests", *Comput. Struct.*, **32**, 609-624.
Tedesco, J. W., Ross, A. C., McGill, P. B. and O'Neil, B. P. (1991), "Numerical analysis of high strain rate concrete tension tests", *Comput. Struct.*, **40**, 313-327.
Tedesco, J. W., Powell, J. C., Ross, A. C. and Hughes, M. L. (1997), "A strain-rate-dependent concrete material model for ADINA", *Comput. Struct.*, **64**, 1053-1067.
Thabet, A. and Haldane, D. (2001), "Three-dimensional numerical simulation of the behaviour of standard concrete test specimens when subjected to impact loading", *Comput. Struct.*, **79**, 21-31.
van Mier, J. G. M. (1986), "Multiaxial strain-softening of concrete", *Mater. Struct., RILEM*, **19**(111), 179-200.
van Mier, J. G. M., Shah, S. P., Arnaud, M., Balayssac, J. P., Bassoul, A., Choi, S., Dasenbrock, D., Ferrara, G., French, C., Gobbi, M. E., Karihaloo, B. L., Konig, G., Kotsovos, M. D., Labnz, J., Lange-Kornbakm D., Markeset, G., Pavlovic, M. N., Simsch, G., Thienel, K.-C., Turatsinze, A., Ulmer, M., van Vliet, M. R. A. and Zissopoulos, D. (1997), (TC 148-SSC: Test methods for the strain-softening of concrete), "Strain-softening of concrete in uniaxial compression", *Mater. Struct. RILEM*, **30**(198), 195-20.
Willam, K. J. and Warnke, E. P. (1974), "Constitutive model for the triaxial behaviour of concrete", *Seminar on*

Concrete Structures Subjected to Triaxial Stresses, Instituto Sperimentale Modelie Strutture, Bergamo, May, Paper III-1.

Winnicki, A., Pearce, C. J. and Bicanic, N. (2001), "Viscoplasic Hoffman consistency model for concrete", *Comput. Struct.*, **79**, 7-19.

CC